Portland State University
PDXScholar

Dissertations and Theses

1-1-2011

Prediction of Soil Layer R-Value Dependence on Moisture Content

Ziyang Liu
Portland State University

Let us know how access to this document benefits you.

Follow this and additional works at: http://pdxscholar.library.pdx.edu/open_access_etds

Prediction of Soil Layer R-Value Dependence on Moisture Content

by

Ziyang Liu

A thesis submitted in partial fulfillment of the
requirements for the degree of

Master of Science
in
Mechanical Engineering

Thesis Committee:
Graig Spolek, Chair
Derek Tretheway
Huafen Hu

Portland State University
©2011

Abstract

This study focuses on how green roof thermal performance is affected by the soil moisture in summer condition. It aims to determine whether moist soil is a better insulator during the summer months than dry soil.

A soil model is developed to predict simultaneous conduction, convection, and surface evaporation for a layer of moist soil representing a green roof. It used to analyze evaporation process and its affect on the soil resistance. The model considers only bare soil without vegetation on the roof. The model predicts the soil surface temperature as it is affected by soil moisture content, which can then be used to calculate heat transfer through the soil layer. An experimental dry out test was conducted to measure the soil moisture and soil temperature histories. Comparison of the predicted and measured sol surface temperature shows that the model reasonably captures the actual behavior. The evaporative cooling effectively reduces the soil surface temperature and heat flux in moist soil and can be used as an effective way to insulate the roof.

Acknowledgement

I would like to thank all the people who helped me, encouraged me and inspired me. This thesis would not have been possible without all your help and support. Foremost, I owe my deepest gratitude to my dedicated advisor, Dr. Graig Spolek for his support of my study and research, for his able guidance, wisdom and patience. I feel sincerely thankful to him being my advisor, who always believe in my potential and encourage me. He is not only my academic advisor, but also a mentor for life. Besides, I am extremely grateful to the rest of my thesis committee: Dr. Derek Tretheway and Dr.Huafen Hu., who give me very important advice for my thesis. Also, I thank all my lab mates at the Green roof Lab. Thanks to Eduardo Guerrero, Debbie Beck, Bryce Cox, Harriet Bell, Giorgina Castillo, Lisa, for that you all made our lab a nice place to work and study. I especially want to show my appreciation to my family for their care and unconditional love. I am indebted to my Mother and Father, Shuhua Ding and Kecheng Liu, who always back up for me. Last but not least, special thanks should go to my dear friends: Wen Fang, Wen Yang, Xiaofang Lu, Jiali Ju, Chengyu Xin, and Hank.

Table of Contents

List of Tables

List of Figures

Introduction

Green roofs are rooftops which are covered with vegetation. This technology has been in existence since ancient times. The first known historical references to manmade gardens above grade were the ziggurats (stone pyramidal stepped towers) of ancient Mesopotamia, built from the fourth millennium until around 600 B.C. Ancient green roof can be found in France, Norway and New York (Theodore.1999). Some of them are still in use today.

Nowadays, green roofs have been installed across America in steadily increasing numbers over the past decade, and research is being conducted in universities on the impact of green roofs on the environment, the economy, and energy conservation. Overall growth from 2007 to 2008 of the North American Green Roof Industry in 2008, compared to 2007, is 35 percent (Green Roof Industry Survey).

Description of systems

The green roof industry has developed two general classifications for rooftop vegetation systems: extensive and intensive; see Figure 1.

Figure 1 Intensive roofs (right) and extensive roofs (left)

The extensive green roof is installed on flat and shallow pitched roofs. Commonly, it contains only one or two plant species with low maintenance like grass and minimal planting medium. It is commonly designed for maximum thermal and hydrological performance and minimum weight load while being aesthetically pleasing. Typically, only maintenance personnel have access to this type of roof.

The intensive green roof contains a variety of plant types. Some rooftop gardens support fairly large trees and water features requiring substantial structural reinforcement. The depth of an intensive green roof is usually greater than an extensive, green roof. Generally, the roof has the public access.

Most green roofs are comprised of five layers. From top to bottom, the layers are plants,

growing medium, a drainage layer, a root barrier, and a waterproofing layer. Under the

waterproofing membrane is the conventional rooftop. Figure 2 shows the green roof

component.
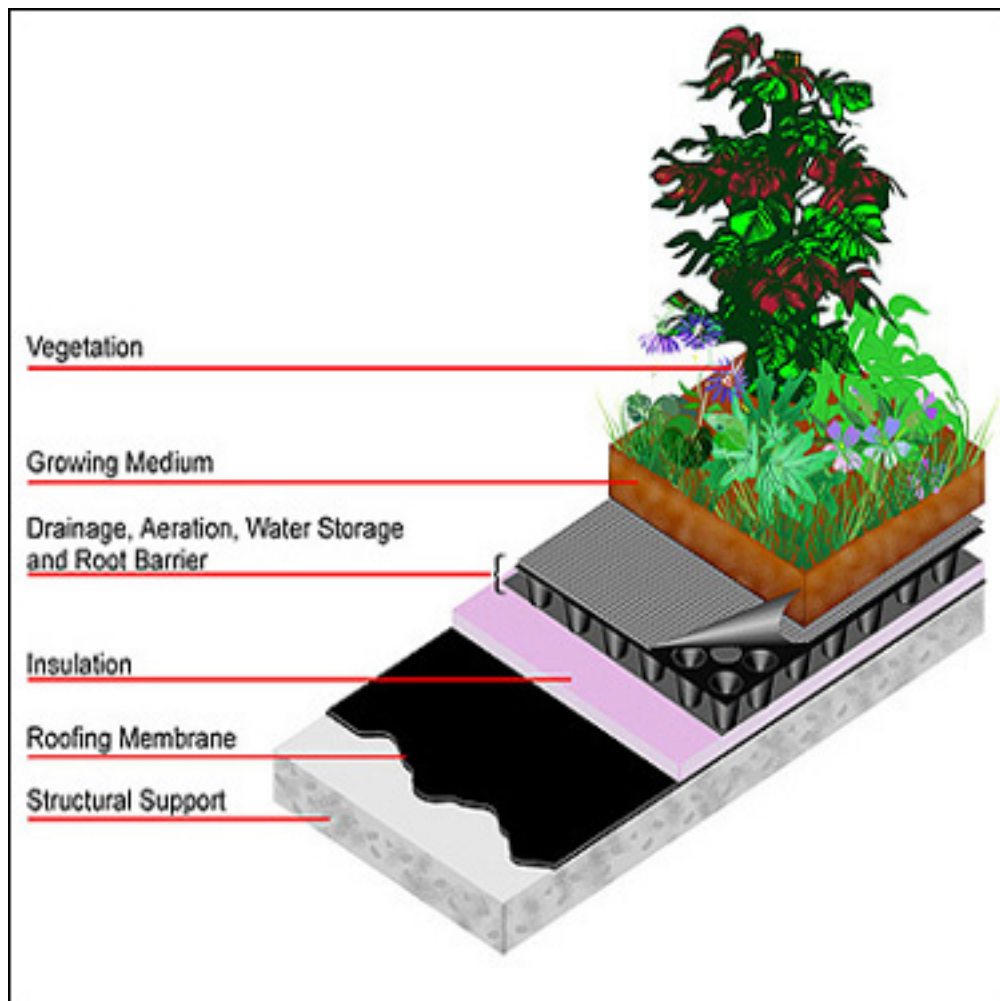
Figure 2 The basic components of a green roof system

Green-roof benefits

In an urban heat island, the temperature of metropolitan areas is higher than surrounding areas. This is due to city building materials absorbing and retaining more heat from the sun rays and the city area lacking vegetation to evapotranspire which can absorb the heat from surrounding areas to reduce the air temperature. The other reason is that energy usage for air conditioning generates waste heat which is emitted to outdoor air. The urban heat island effect can change weather patterns, causing smog development and increasing precipitation. Also, the effect can adversely affect human health. Using green roofs can effectively improve the urban heat island effect, due to the potential to decrease the surrounding air temperature by plants transpiration. Lawrence Berkeley Laboratory has shown that a 5% increase in green space in a large metropolitan area would reduce the average summer time temperature by 4 F, and would reduce smog by 10% (Perry 2003).

A green roof can effectively moderate the temperatures of the building, due to the shading of sunlight by the plants, the insulation of the soil, and the cooling effect of evapotranspiration. The study of the National Research Council of Canada showed that in summer time a green roof surface temperature can be 30 °C compared to a reference roof temperature of 70 °C. Additionally a green roof's mean daily temperature fluctuation is 5-7 °C, while the reference roof is from 42 to 47 °C. By moderating the roof

temperature, the heat flux into the building is reduced. This means the cooling demand can be reduced (Liu 2003).

Green roofs systems often help solve the problem of storm water runoff. When a city has precipitation, the over flow water puts pressure on the city sewer and drainage system. It can cause flooding, erosion, sewage back up, and pollution of water supplies system. Green roofs can retain about 70% to 90% of the rainfall, which stabilizes water runoff and relieves overloaded drainage systems (Perry 2003). A 2002 National Research Council of Canada (NRCC) project found that a green roof could delay storm water run off and reduce peak run off rate and volume. The study found that the green roof retained 245mm out of the 450 mm of rain fell during April to September 2002; this is a reduction of 54% (Liu 2003).

The green roof technology can bring additional positive impacts to the city. First, it can make a city aesthetically pleasing.

Figure 3 shows the rooftop garden in a Japan shopping mall called Namba Park. Second, plants can reduce pollution by collecting dust and other pollutants and reemitting oxygen (Perry 2003). The green roofs produce a substantial about of oxygen for an urban area.

Figure 3 Namba park rooftop garden view

Chapter 2 Literature review

Presently, green roof performance is a priority research focus. Researchers build green roof models, using software like Energy Plus (Sailor D. 2008) or eQuest to simulate the green roof performance. Others gather experimental data on green roofs in the field or lab.

Del Barrio(1998) proposed a green roof energy model with three major parts: the roof support, the soil, and the canopy. The model combined the three layers together to simulate the energy performance recorded during a climate data test in Athens in August 1982. It takes a series sensitivity analysis on the canopy and green roof.

In the soil component, the primary factor is the heat flux variation with changes in soil depth, soil density and water content. The model calculated the heat flux with respect to two different soil water contents 20% and 40% respectively. When the moisture content in the soil increased, the heat flux through the roof was reduced.

Takakura(2000) investigated the cooling effects of plants on buildings via modeling and simulation. They concluded that evapotranspiration was a very important factor in cooling ability of green roof but that accurate measurement of the evapotranspiration is impossible.

Kunar, Kaushik(2005) developed a mathematical model to determine the effects of leaf area index(LAI is the total leaf surface area contained in a volume of unit base) and plant height on the green roof's thermal performance. This model was built to improve upon Del Barrio's model. The model was validated by experimental data measurements from an existing green roof in Yamuna Nagar, India. It concluded that the green roof combined with solar thermal shading reduced averaged indoor air temperature by 5.11°C, from the average indoor air temperature for the bare roof. This suggests that a larger LAI reduces the canopy air temperature, stabilized the fluctuating values and reduced the penetrating flux. Here，the focus was on green roof shading effect.

Ondimu and Murase(2007) combined finite-element modeling and neural networks analysis together to determine the thermal conductivity of a sunagoke moss mat. Sunagoke moss is a living biological material fabricated from sumagole moss, cotton wool and PVC netting. The model considered three different moisture contents: 0%, 50%, and 100%. The material's R-value is higher when dry vs. wet.

Lazzarin, et al(2005) designed a green roof model using the finite difference method to perform an energy balance on each layer. Data was acquired from a green roof on an Italian hospital in 2002 and 2003. It analyzed the different heat performance for a dry green roof, a wet green roof, and a traditional roof in summer and winter. It concluded that evapotranspiration is very important with the model predicting better performance in well-watered conditions. Figure 4 shows the energetic exchanges of the green roof and traditional roof in summer.
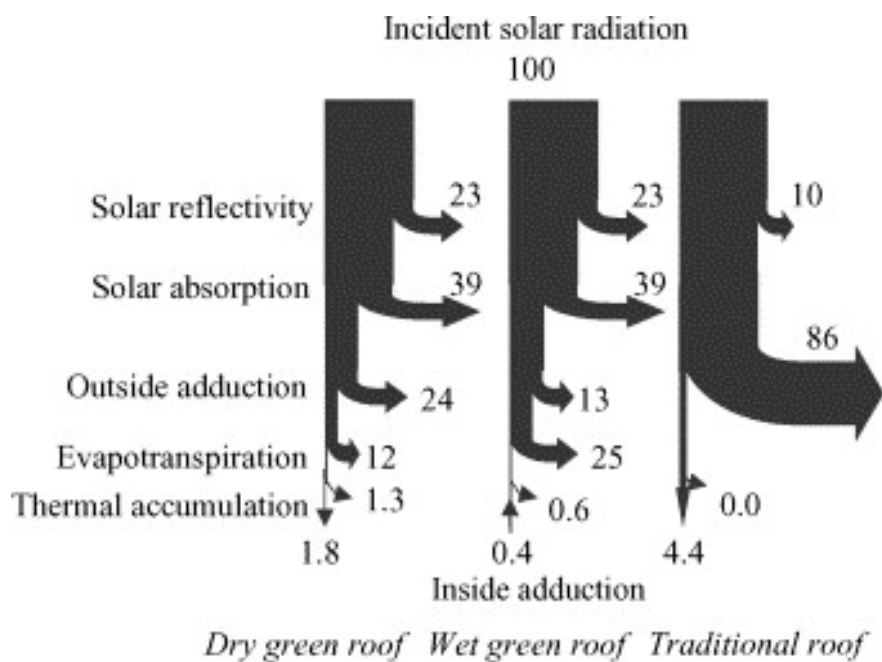

Figure 4 Comparison of the energetic exchanges of the dry or wet green roof with a traditional roof, starting from 100 incident solar irradiation units-summer session. (Lazzarin, et al.2005)

9

Feng and Meng(2010) created a model to consider the green roof model and added plant metabolism, specifically photosynthesis and respiration. An equation simply determined the solar energy converted by net photosynthesis. From the field experiment 9.5% of dissipated heat was by due to the net photosynthesis of plants. The most important part is evapotranspiration which is 54.8%.

As green roof heat performance becomes more and more important, some disputes have occurred.

Early studies like Curtis (1936), Mellor, et al(1964) revealed that the thermal radiation from leaves was the key factor in reducing the heat transferred into the rooms beneath. But Wong, et al(2003), Theodosio (2003), Barrio (1998), Takakura, et al(2000), Onmura, et al(2001) studied the energy balance of green roofs and concluded that the dominant method for absorbed heat to dissipate was evapotranspiration.

Medjelled, et al(2008) built a mathematical model that predicted the unsaturated underground soil U-value at different moistures. They developed a small scale underground heat storage system to get the test data. The model was affected by the conduction heat transfer only. As the thermal conductivity increased with the increase

in moisture，the soil U-value also went up. This is consistent with the effect of green roof soil moisture on thermal conductivity as measured by Sailor, et al (2008)

Alcazar and Bass (2005) compared the energy performance of a multi story residential building in Madrid using three different roofing systems: a common flat roof, a green roof and a green roof with water storage capacity. In the study, the moisture content in the soil ranged from 0% to 100% (saturation level). Use ESP-r modeled two values of moisture content 20%, 80%; ESP-r is an integrated modeling package for the simulation of the thermal performance of buildings. Table 1 shows the overall conductance values U and Resistance (R-value) for all three systems with 0%, 20%, and 80% moisture content. As shown in the table, the moisture content in the soil has a significant effect on R-value, which is the inverse of the conductance U. An increase in moisture content in the soil from 0%-20% produces a decrease in the soil R-value from 0.67 to 0.11m2°C/W, an 84% decrease.

Table 1 Effect of soil moisture content on green roof R-value and U-value (Alcazar and

Bass 2005)

	κ(W/m°C)	C (W/m²°C)	R soil (m²°C/W)	BGR U(W/m²°C)	BAR U(W/m²°C)
soil substrate (0% moisture)	0.15	1.49	0.67	0.42	0.38
soil substrate (20% moisture)	0.19	2.12	0.47	0.46	0.41
soil substrate (80% moisture)	0.8	9.10	0.11	0.53	0.48

R:Thermal resistance; BGR: Building with the Green roof; BAR: Building with the Aljibe Roof

Wong, et al.(2003) used the DOE-2 software to simulate the peak roof thermal transfer

value, which is the square roof of peak sensible cooling for roof component. The R-value

of dry and 40% moisture content clay soil of different thickness are shown in Table 2.

The R-value is greater when the soil moisture content decreases.

Table 2 R-value of different soil thickness with different moisture content (Wong, et al.

2003)

Soil thickness (mm)	Clay soil (dry) R-values (m² K/W)	Clay soil (40% moisture content) R-values (m² K/W)
100	2.349	2.012
200	2.749	2.076
300	3.149	2.139
400	3.549	2.202
500	3.949	2.266
600	4.349	2.329
700	4.749	2.392
800	5.149	2.455
900	5.549	2.519

From Del Barrio (1998)'s soil model, one can estimate the green roof insulation affect on the thickness of the soil layer, density, and moisture content. As the density decreased from 1500 to 1100kg/m3, the soil thermal conductivity decreased, and heat flux through the roof decreased. In addition, the moisture content decreased from 40% to 20%, which means the thermal conductivity decreased. However, the heat flux through the roof increased. The augmentation of surface soil evaporation is a contributing factor.

Tabares-velasco (2009) ran the green roof thermal performance test under laboratory condition; he found that as the soil water content increased the latent heat flux increased, but the total heat flux decreased.

Clearly, modeling and experimental results reported in the literature disagree on the effect of soil moisture on green roof heat flux. The dispute over whether the R-value of moist soil is greater or less than the dry soil has not been settled conclusively. Prediction of the R-value at different moisture level is complicated. The presence of moisture could increase the soil thermal conductivity since water is a better conductor than air in the voids. This mean the R-value of the soil should decrease. But when the soil is moist, evaporative cooling will be enhanced. Evaporative cooling occurs as evaporative latent heat, which is the thermal energy required to cause a phase changes from water to vapor. As the surface of the soil dries, the capillary force will pull more moisture from

the soil below. But as the soil dries out, evaporative cooling decreases, so the effective thermal resistance diminishes.

Likely, there should be some combination of both effects as shown in Figure 5. It is unknown which factor will affect the soil layer R-value more, as it is unknown if the presence of more moisture in the soil would increase or decrease the ability for heat transfer.
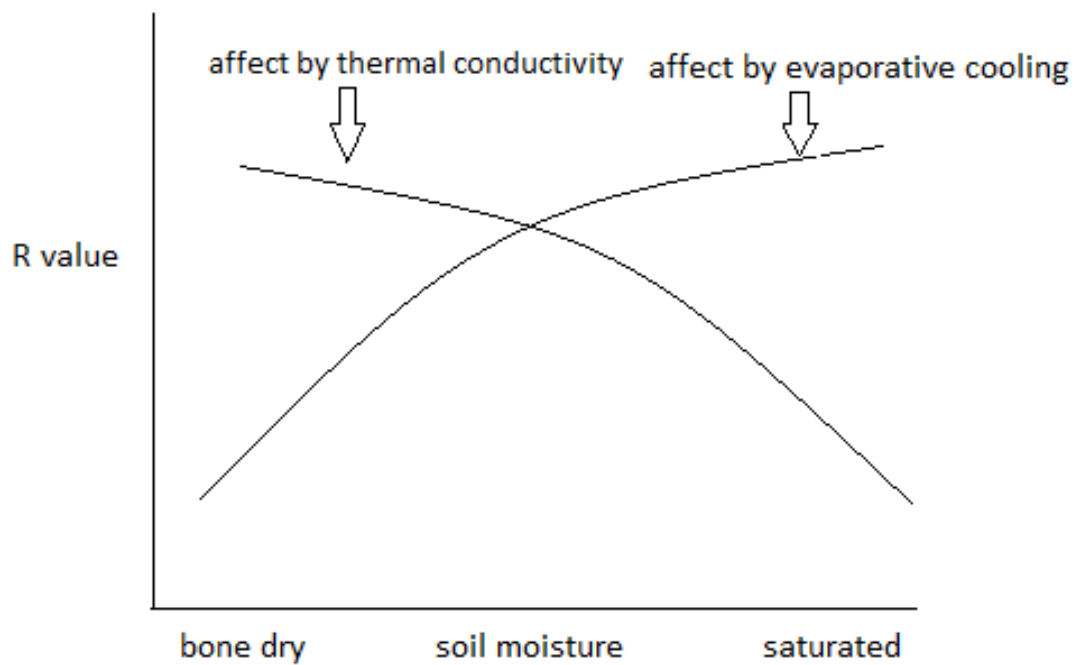

Figure 5 Two factors affecting the soil R-value

Chapter 3 Project Objective

The objective of this study was to develop a soil model based on thermal performance analysis which included the effect of soil moisture on evaporative cooling and conduction. The model considered only bare soil without the complicating effects of green roof plants. Model predictions were validated by experiment.

Chapter 4 Theoretical Model

Physical Model

Heat transfer processes taking place on a green roof are conduction, convection, net radiation, evapotranspiration, thermal storage for the substrate, and metabolic storage (photosynthesis and respiration).

Conduction is the transfer of thermal energy between neighboring molecules in a substance due to a temperature gradient. In the summer season, the heat flux transfers from hot ambient air through the building roof top to inner conditioned space. For the green roof, the heat flux goes from top to bottom as the temperature gradient occurs.

Three things affect the rate at which soil conducts heat: the soil depth, the thermal conductivity, and temperature difference. Soil thermal conductivity, in turn, is affected by four factors: moisture content, density, composition and temperature. Of these, moisture content has the greatest impact on the soil's thermal conductivity. When water is added to bone dry soil, a thin water film covers the soil particle, which creates air gaps between the small soil particles. In other words, it can increase the effective contact area between the soil particles, thus increasing heat flow, resulting in higher thermal conductivity. Soil thermal conductivity also increases with the dry density of the

16

soil. With an increase in dry density, more soil particles are packed into a unit volume and the number of contact points between the particles increases. This increase in contact points provides a larger heat flow path and increases the soil thermal conductivity (Becker, 1992).

Evapotranspiration is a term used to describe the sum of soil evaporation and plant transpiration from a vegetated surface to the atmosphere. For water to change its state from a liquid to a vapor, it requires absorption of energy. In a green roof, water that is contained in the soil and in the plant evaporates into the surrounding air. When water is released to the surrounding air in the form of vapors, evaporative latent heat is drawn from the surrounding air and soil. For a soil bed without plant, soil moisture is evaporated from the water filled surface pores.

The evaporation rate is the quantity of water evaporating per unit of time. As an initially moist bed of soil dries out, the drying rate can be divided into three stages: the constant-rate, the falling-rate, and the low-rate stages as illustrated in Figure 6 (Suleiman and Ritchie,2003). The constant-rate stage represents the period when soil water is not limiting the evaporation rate; the evaporation rate is determined by the available energy at the surface by convection and atmospheric conditions (relative humidity, temperature, and wind velocity). During this stage, the evaporation rate

would be constant if the energy supply and atmospheric conditions are in a steady state. In contrast, water loss from a soil with a dry surface layer is regulated primarily by soil water resistances that limit the rate at which water moves upward to the evaporating surface (Philip,1957). This causes the falling-rate stage. It represents the period when the evaporation rate is jointly controlled by the soil water supply to the surface, the energy supply, and atmospheric conditions. During this stage, the rate of supply of water to the surface from the soil below decreases, causing the surface water content to become drier. In such a case, the surface layer cannot continue to provide enough water from storage, and the evaporation rate becomes limited by the rate of water movement to the soil surface. During this stage, the evaporation rate gradually decreases. The low-rate stage represents the final period when the evaporation rate is controlled by the soil's physical characteristics. This can take a long time, as the evaporation rate is much less than the constant-rate stage.
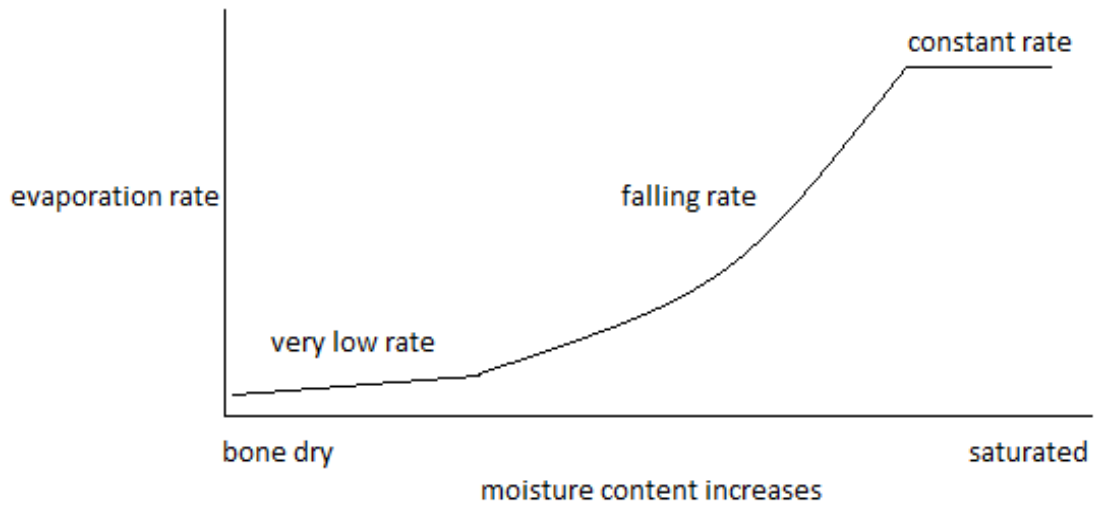
Figure 6 Soil evaportaion three stage changes by soil moisture content

For an extensive green roof model, the soil layer is relatively thin, so it may not hold enough water for constant rate evaporation. Although some regions have large precipitation, most of the water drains off due to thin soil layers. A model of energy transfer in a thin layer of moist soil must allow for variable drying rate (evaporation rate) as moisture content changes.
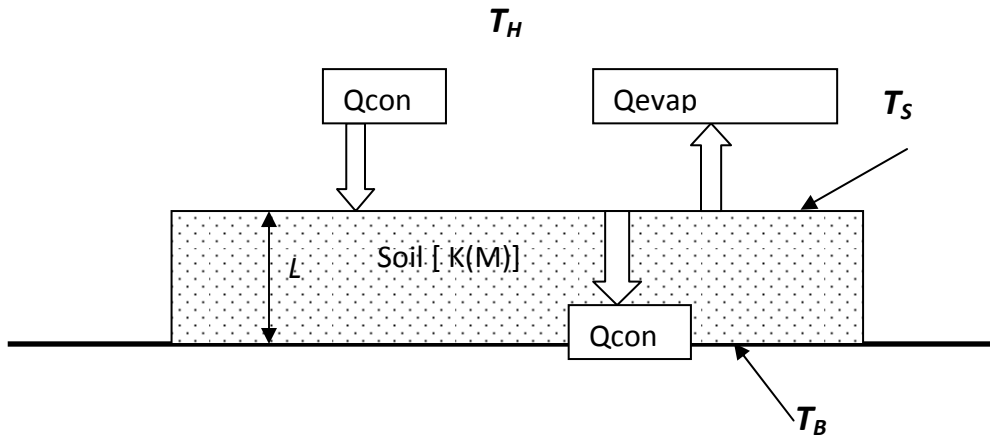
Figure 7 Soil layer energy balance model

Figure 7 shows three heat transfer process take place the soil layer. Conduction heat transfer allows heat flux from the soil surface to the bottom, convection transfers heat from the hot ambient air to soil surface, and evaporative cooling cools the soil surface and ambient air temperature.

Mathematic Model

From the soil energy balance diagram, the soil balance heat equation is:

$$Q_{cond} + Q_{evap} = Q_{conv} \tag{1}$$

Q_{cond} = the conduction heat flux in W/m2

Q_{evap} = soil surface heat flux from evaporation W/m2

Q_{conv} = the convection heat flux in W/m2

The assumptions used to develop this model are:

1. The soil area is large enough to assume horizontal homogeneity and heat and mass fluxes are assumed to be mainly vertical, so one-dimensional models can be used to describe the thermal performance by applying one-dimensional (vertical) analysis.

2. The soil layer is thin enough to assume the whole soil layer's water content is uniform. Therefore, the soil layer's thermal conductivity is also uniform.

3. The soil is homogeneous.

4. As the soil layer is drying out, heat transfer and mass transfer are decoupled so that heat transfer can be assumed to be steady state while moisture transfers in transient.

5. Radiation, both short and long wave, can be included in the convective heat transfer.

Conduction:

The fundamental one-dimensional conduction equation is as follows:

$$Q_{cond} = k \frac{T_S - T_B}{L}$$

(2)

Q_{cond} = the conduction heat flux in W/m2

T_S = soil surface temperature in ℃

T_B = soil bottom temperature in ℃

k = soil thermal conductivity W/m℃

L = soil layer thickness in m

Conductivity varies with soil water content: $k = k(\theta)$

θ = volumetric soil water content in %

Convection:

$$Q_{conv} = h_{eff} (T_H - T_S)$$

(3)

Q_{conv} = the convection heat flux in W/m2

h_{eff} = effective convection coefficient in W/m2℃

T_H = hot air temperature in ℃

T_S = soil surface temperature in ℃

Evapotranspiration:

$$Q_{evap} = \dot{m}h_{fg}$$ (4)

Evaporation rate varies with soil water content:

$$\dot{m} = \dot{m}(\theta)$$

Q_{evap} = soil surface heat flux from evaporation W/m²

$\dot{m}$ = soil surface evaporation rate W/m²

h_{fg} = latent heat kJ/kg

In steady-state conditions, an energy balance equation for soil's surface yields

$$Q_{in} = h(T_H - T_S)$$ (5)

$$Q_{out} = k\frac{T_S - T_B}{L} + \dot{m}h_{fg}$$ (6)

When energy balance occurred at soil layer surface

$$Q_{in} = Q_{out}$$ (7)

Solving for T_S

$$T_S = \left[\frac{1}{1+Bi}\right]\left[T_B + BiT_H - \frac{L}{k}\dot{m}h_{fg}\right] \qquad (8)$$

Where Biot Number $Bi = hL/k$

Model Examination

The soil surface temperature is affected by conduction, convection and evaporation. To compare the model with and without evaporative cooling effect, setting $\dot{m}$ is set to zero.

$$T_S = \left[\frac{1}{1+Bi}\right]\left[T_B + BiT_H - \frac{L}{k}\dot{m}h_{fg}\right] \qquad (8)$$

which yields,

$$T_S = \frac{BiT_\infty + T_B}{(1+Bi)} \qquad (9)$$

Although the evaporation rate is ignored, the thermal conductivity is affected by the moist soil. Soil thermal conductivity (K) increases with increase moisture. When soil is totally dry, K is small. Thus, Bi is large, and T_S is close to T_∞. At steady state, the surface temperature is close to the hot air temperature. When the soil is saturated, K is quite large, and Bi is small. T_S approaches T_C. This is an extreme condition that surface temperature affected most by cold side conduction.

Next, add the evaporation term in the equation. Under ideal conditions, the surface soil layer is always saturated due to capillary pressure. The capillary flow rate is greater than the evaporation rate, so the evaporation process is at a constant rate. Assuming latent heat is constant, the evaporation term is constant, and the model changes to:

$$h(T_\infty - T_S) - Q_{evap} = \frac{K}{L}(T_S - T_B) \tag{10}$$

Solving for T_S

$$T_S = \frac{BiT_\infty + T_B - C}{(1 + Bi)} \tag{11}$$

With $C = Q_{evap} \dfrac{L}{K} > 0$

From the new surface temperature equation, the surface temperature will be lower than the surface temperature without evaporative cooling effect. This is because evaporation requires absorption of heat, which cools down the soil surface temperature. As the soil moisture goes up, T_S have a similar trend like T_S without evaporation.

Actually, the soil layer of green roof cannot remain saturated continuously. For most granular materials, evaporation rate slows down as the soil water content decreases. So the evaporation rate is a function of soil water content. The surface temperature equation is:

$$T_S = \left[\frac{1}{1+Bi}\right]\left[T_B + BiT_H - \frac{L}{k}\dot{m}h_{fg}\right]$$ (8)

Where $\dot{m}$ decreases with decreasing θ

Compared to the constant evaporation rate, as the moisture content increases, the evaporation term grows. The Figure 8 shows this hypothetical relationship between soil water content and T_S. T_S curve with soil moisture increase is greater than the constant evaporation rate case T_S curve and less than on evaporation rate case T_S curve. For bone dry soil, T_S equals T_S without evaporation.
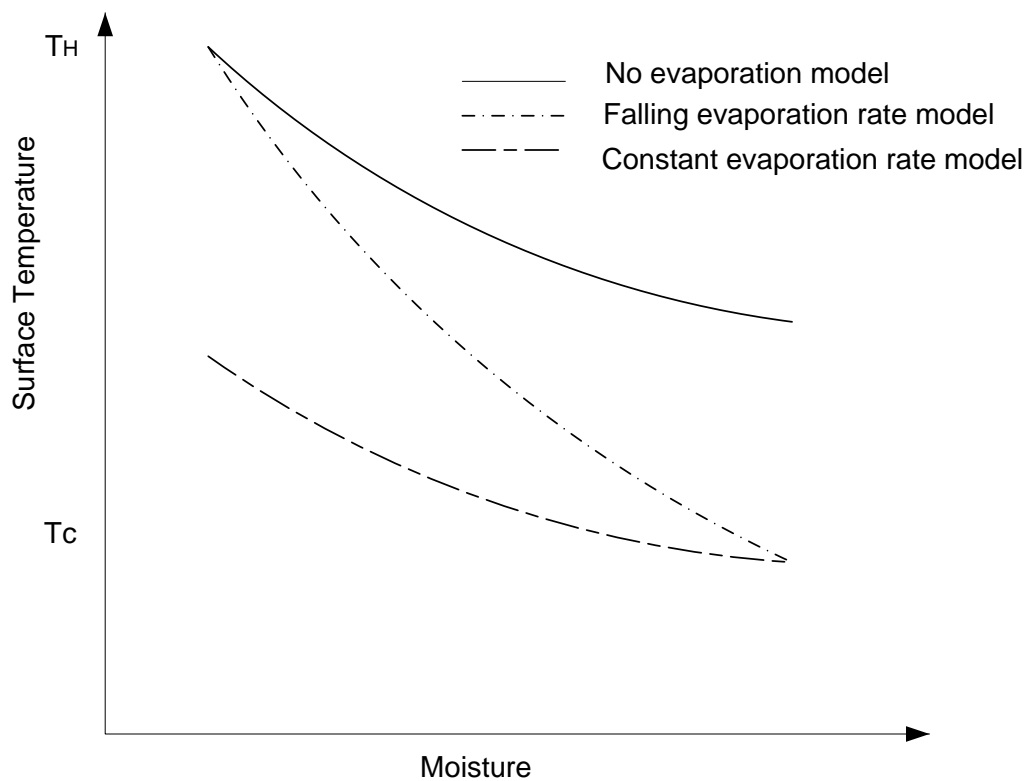

Figure 8 Surface temperature model changed by soil moisture content

26

Chapter 5 Experimental Methods

An experiment was performed to validate the energy balance model described above and analyze the energy flow of typical extensive green roofs without plants. To avoid the unsteady-state condition, the experiment was conducted inside a controlled environment (Bell and Spolek 2008).

Based on $T_S = \left[\dfrac{1}{1+Bi}\right]\left[T_B + BiT_H - \dfrac{L}{k}\dot{m}h_{fg}\right]$

(8) where $k = k(\theta)$ and $T_S = T_S(\dot{m},\theta)$, for constant L, h, TH, and hfg, two separate experiments were performed.

5.1 Thermal conductivity test

In this test, a KD2 Pro dual probe sensor from Decagon Device was used. The dual probe has two parallel needle probes separated by a distance of 6mm. The needles are 1.3mm in diameter and are 30mm long. One probe contains a heater and the second probe is the temperature sensor. The dual probe device is inserted into the soil, and for measuring the thermal conductivity, a heat pulse is applied.

The device uses a transient heated needle and an approximation to the solution of the differential equation for an infinite heat source as the method for finding thermal conductivity.

For heat rate Q, the solution for the different equation for finite length 2b and cylindrical probes with radius a is given by (KD2 Pro manual, 2006)

$$\Delta T = \frac{q}{4\pi k} \int_{r^2/4Dt}^{\infty} u^{-1} \exp(-u) \exp[-(a/r)^2 u] I_0 (2au/r) erf(\frac{b}{r}\sqrt{u}) du \tag{11}$$

Where $I_0(x)$ is a modified Bessel function of order zero, $erf(x)$ is the error function, and u is the integration variable.

The double probe thermal conductivity device was used to test the soil thermal conductivity over a wide range of soil water content from bone dry to fully saturated.

To test the water holding ability of soil, soil was dried in an oven until bone dry. A container with known volume (VT) and a small hole on the bottom was filled with dry soil. Next, water was added into the soil continuously until minor leaking came from the bottom hole. By measuring how much water was added (VW), the volumetric water content was calculated by following equation:

$$\theta = \frac{V_W}{V_T} \tag{12}$$

Where θ is the volumetric water content, V_W is the volume of the water, and V_T is the total soil volume.

Intermediate values of θ between θ_{dry} and θ_S were obtained for the values of V_W. The thermal conductivity for each sample at different water contents was measured with the conductivity device.

5.2 Soil Dry out test

To provide constant heat transfer conditions, a low speed wind tunnel shown in Figure 9 was used, representing warm summer conditions. Hot air was heated by electric heaters and blow through the upper section at a fixed air speed and temperature. Cold air propelled by an air conditioner flowed through the lower part to simulate an air conditioned indoor space beneath a green roof. Two trays with bare soil were placed on the deck between the hot and cold section. Sensor locations are illustrated on Figure 9.

AIR FLOW

HEATING

COOLING

Heat Flux Meter
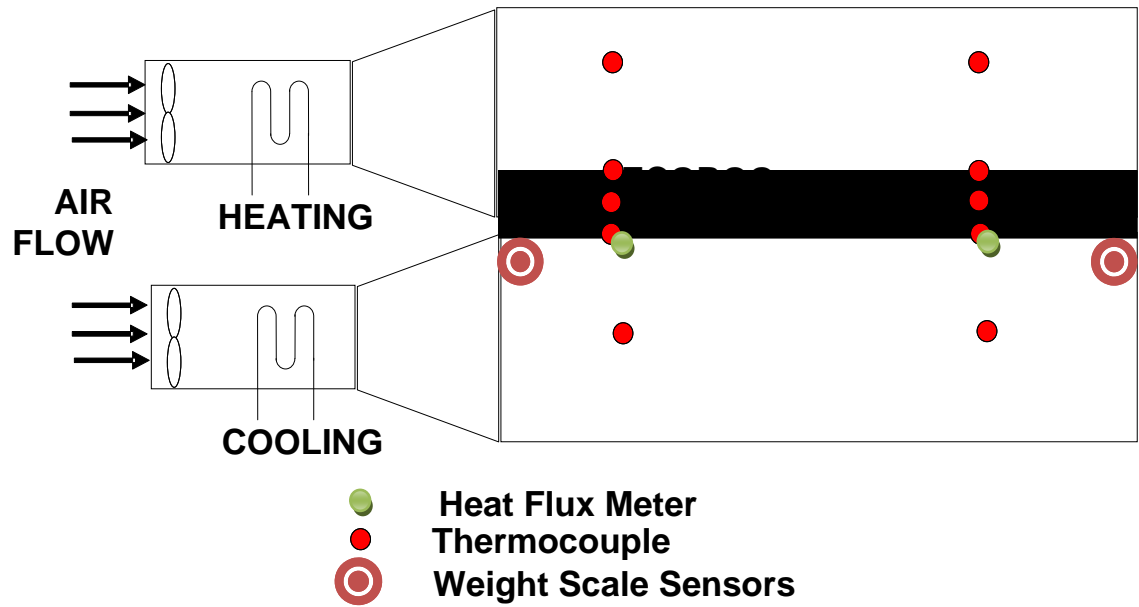Thermocouple
Weight Scale Sensors

Figure 9 The wind tunnel is cross sectional view and photograph

Thermocouples

There are two methods to test the soil surface temperature: (1) IR camera, and (2) thermocouples. Since continuous data was needed for this laboratory test, thermocouples were chosen to monitor the temperature.

A thermocouple consists of a junction between two different metals that will produce a voltage proportional to the temperature difference due to the Seebeck effect. Each type of thermocouple has a well defined voltage output at a certain temperature.

A thermocouple type OMEGA TVC-PC-T-24-180 was used to monitor the temperature. Type T thermocouples are suitable for a temperature range of -250 °C to 350 °C, compared to the experimental range of temperatures of 7 °C to 40 °C. The standard limit of error is ± 1°C.

TH, TC (cold air temperature), TS, TM (soil middle point temperature) and TB were monitored. These were located approximately in the plan area center of tray. The air thermocouples were fixed using adhesive plaster, and the sensor for surface temperature was slightly covered by the surface soil. The thermocouples for the middle soil temperature were held in position with a stick.

Heat flux

Heat flux is the rate of energy passing through a surface per unit area. In the experiment, heat fluxes were directly measured with factory- calibrated heat flux meters. They were applied to the underside of the deck holding the tray and located at the center of the tray.

Load cell sensor

A OMEGA's LC305 Series load cell was set under each of the deck's four corners as shown in Figure 10, to measure the weight of the deck and trays. The weight in the whole test process was used to determine the soil water content changes.
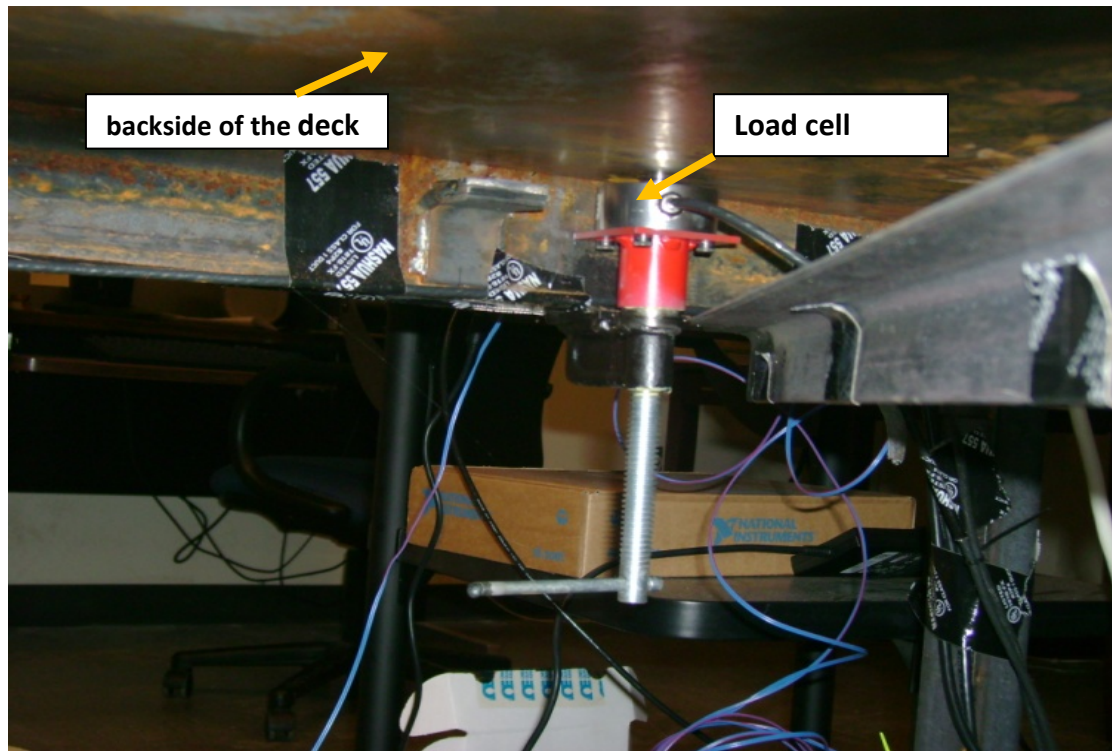
Figure 10 The load cell sensor located on the back side of the deck

The load cell is a transducer that is used to convert a force into electrical signal. Through a mechanical arrangement, the force being sensed deforms a strain gauge. The strain gauge converts the deformation to electrical signals. A load cell usually consists of four strain gauges in a Wheatstone bridge configuration.

Test soil and tray

The size of the tray is 61cm by 58cm in wide and 3cm depth. In this test, the soil was placed directly in the tray without drainage layer and waterproof layer (common in green roofs) to avoid adding thermal resistance. A drain hole was located on the middle of one side to allow excess water to drain when the soil was over saturated, as shown in Figure 11.
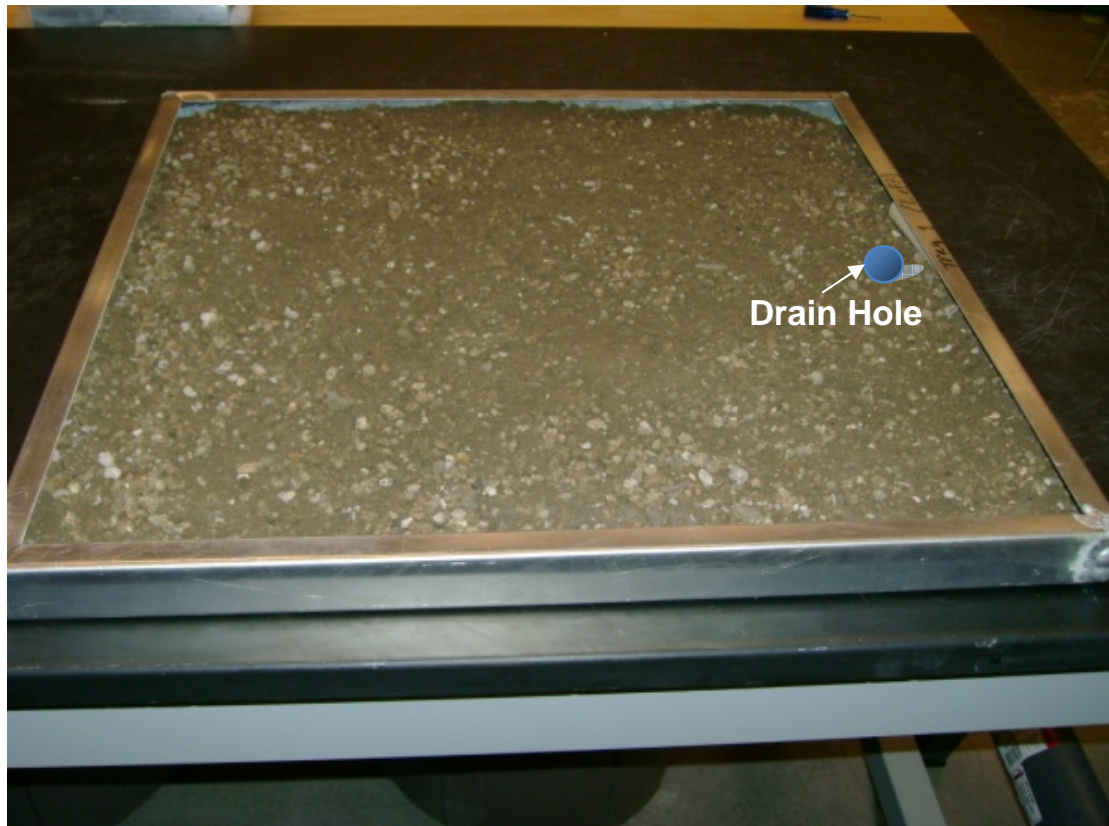

Figure 11 The drain hole location on the tray

The soil was classic Pro-Gro extensive roof top media composed of special screened pumice, fiber life compost, and paper fiber. Fiber life compost is a by-product of a anaerobic digestive process.

Calculation of bare wind tunnel R-value

The deck without tray on it has its own thermal resistance. To test its R-value, thermocouples measured the deck surface temperature and cold side temperature. With the heat flux sensor monitored heat transfer, the test was run for 30 minutes to get a steady state R-value, which was found to be 0.18ft2°Fhr/BTU.

With the wind tunnel R-value test runs, the heat passes through the soil tray and test bed in series. The respective resistances to heat flow is:

$$R_{overall} = R_{deck} + R_{soil}$$

So the net R-value of each test soil tray was corrected with the overall R-value.

Test procedure

Soil trays were initially watered to full saturation, as determined when water stopped draining from the drain hole. Hot air at 40 °C and cold air at 7°C ware applied continually to dry the wet soil. Tests continued until the weight of the soil was almost constant. This

meant the evaporation stage has changed to the third level or the every low-rate soil water content.

In the test the following variables were collected: heat flux, hot temperature, surface temperature, middle temperature, bottom temperature, cold temperature, and weight. Typical tests ran 84 hours to reach approximates steady state condition.

Chapter 6 Results and Discussion

6.1 Experimental Results

Figure 12 shows the soil thermal conductivity linearly increases with the soil moisture. For bone dry soil, the soil thermal conductivity is 0.089W/m K. For saturated soil (θ=0.4), the thermal conductivity is 0.325 W/m K. A least- squared curve fit was generated for model use that predicts:

$$K = 0.104 + 0.557\theta \tag{13}$$

θ is the volumetric moisture content. The regression coefficient $r^2 = 0.977$ indicates that the linear curve fit is a good approximation.
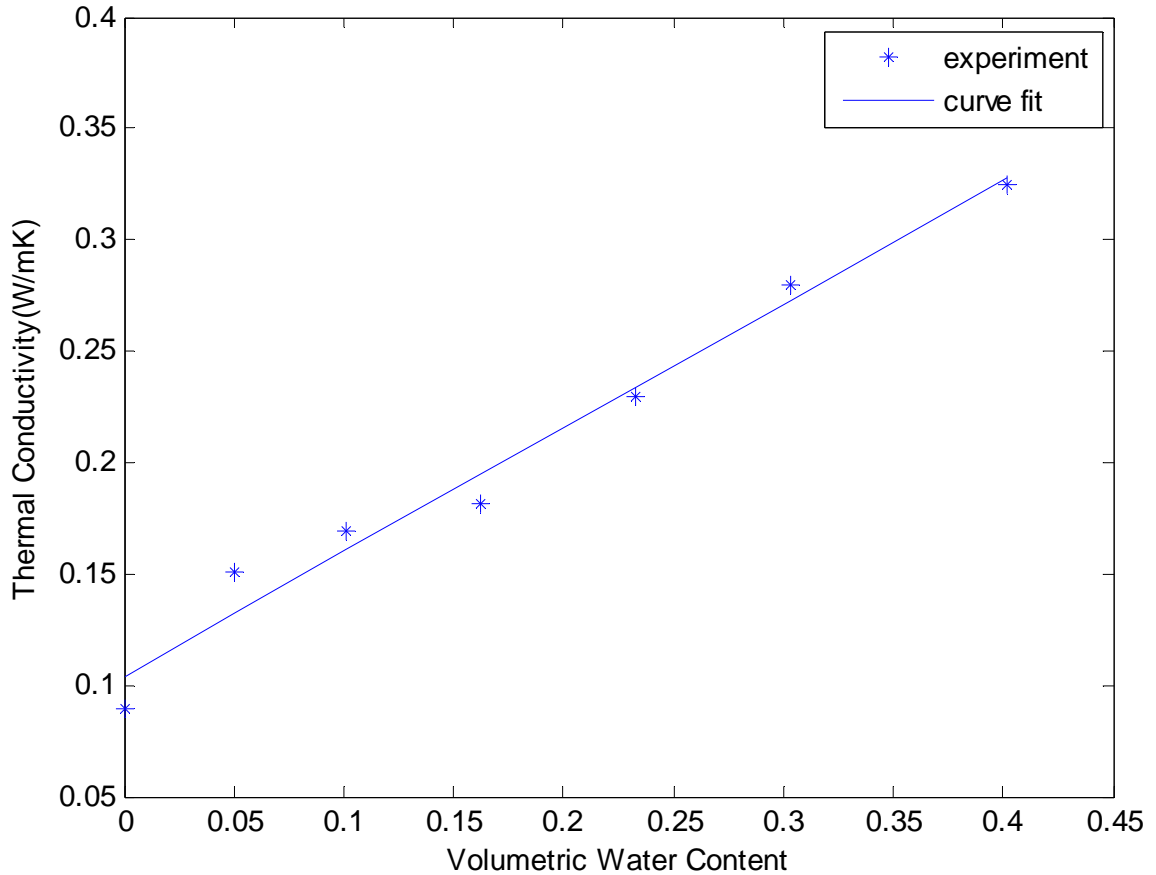
Figure 12 Soil thermal conductivity range from bone dry to saturated

Figure 13 shows the weight change of the soil tray drying out. The solid line is the experimental data and illustrates a signal noise of about ± 0.5lb. In the test, the load cell sensor could only test the total weight, which includes the soil, the water, the tray and the wind tunnel deck. The tare due to the tray and empty decks weight was subtracted to yield the soil and water weight. At the end of 80 hours, the weight changes slowly. The trend line (dashed) in Figure 13 is fitted to the exponential equation

$M = M_f + C_1(M_i - M_f)e^{c_2 t}$, C_1 is the correction coefficient, C_2 is the decay coefficient

M_f is the soil weight after the test, M_i is the initial soil weight, and t is time. From the

data in Figure 13 the equation is $M = 38.33 + 9.33e^{-0.032t}$ (14)

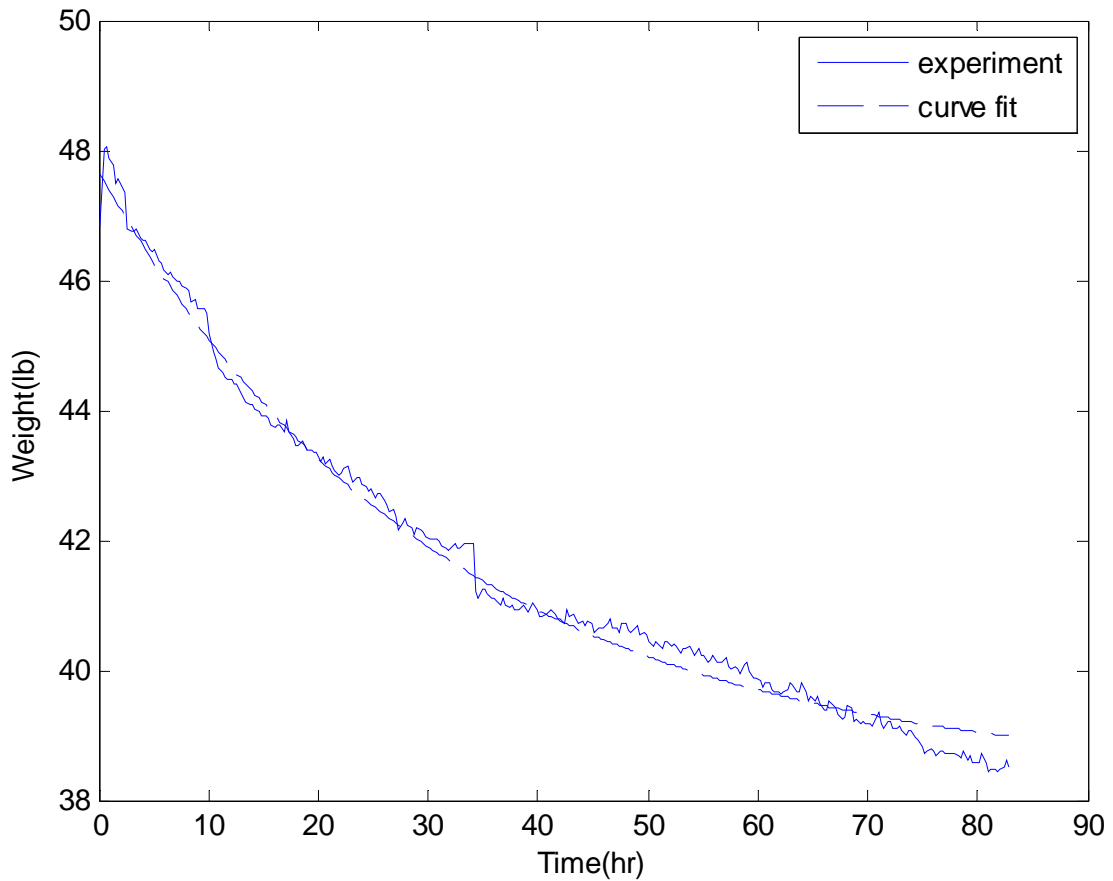It matches experimental results reasonable well.

Figure 13 Soil weight changes with time as the soil dries out due to evaporation.

During the test, water can only diminish by the evaporation (there is no drainage), so the weight change is because of the water evaporation into the air. The evaporation rate was determined as the weight change per unit time. As Figure 13 shows the weight history, the slope of the weight change was found to be $\dot{m} = 0.053e^{-0.032t}$. Where $\dot{m}$ is soil layer evaporation rate in g/s m^2. Figure 14 shows this graphically.
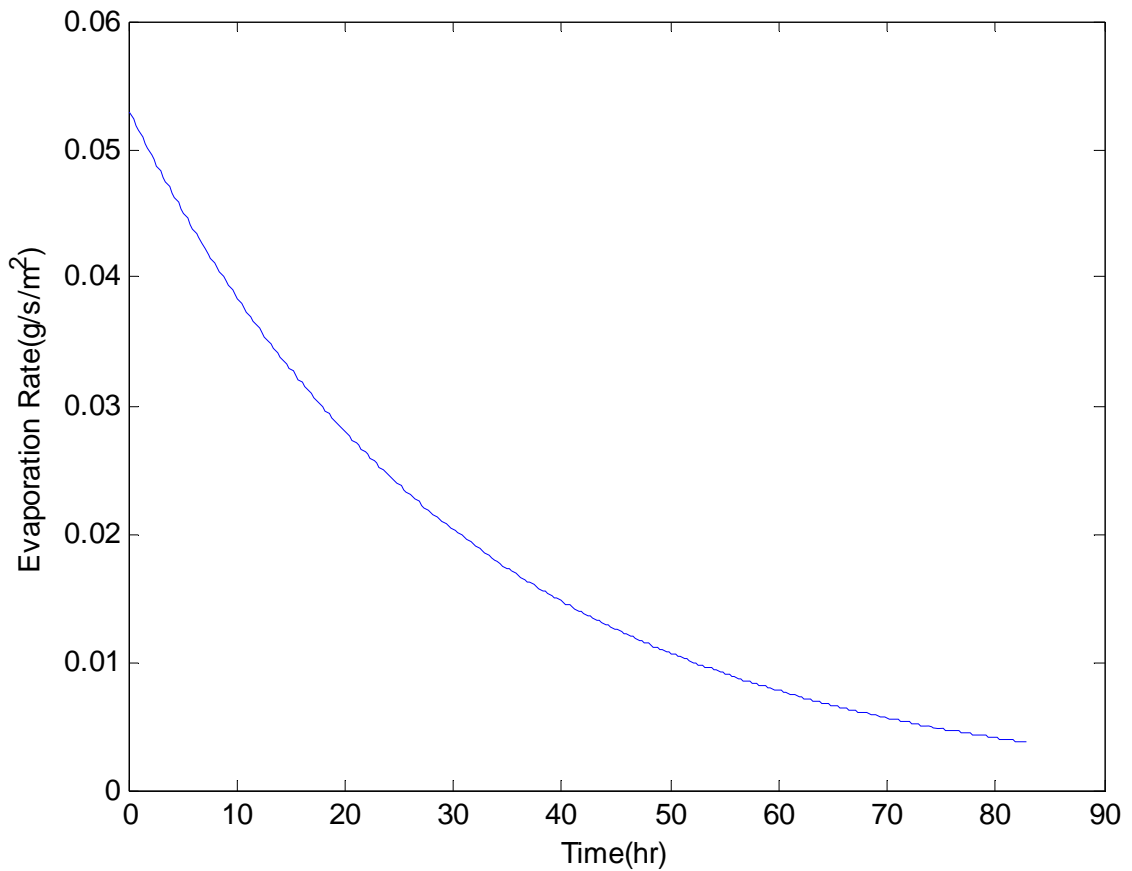

Figure 14 Unit area evaporation rate changes by time

Additionally, the soil volumetric water content was calculated from Figure 13, using the

water content definition $\theta = \dfrac{V_W}{V_T}$, since the water volume could be related to the weight

of the water by its density. The soil volume was determined during filling of the tray.

From Figure 15, the volumetric water content decreases fast at the beginning, and at

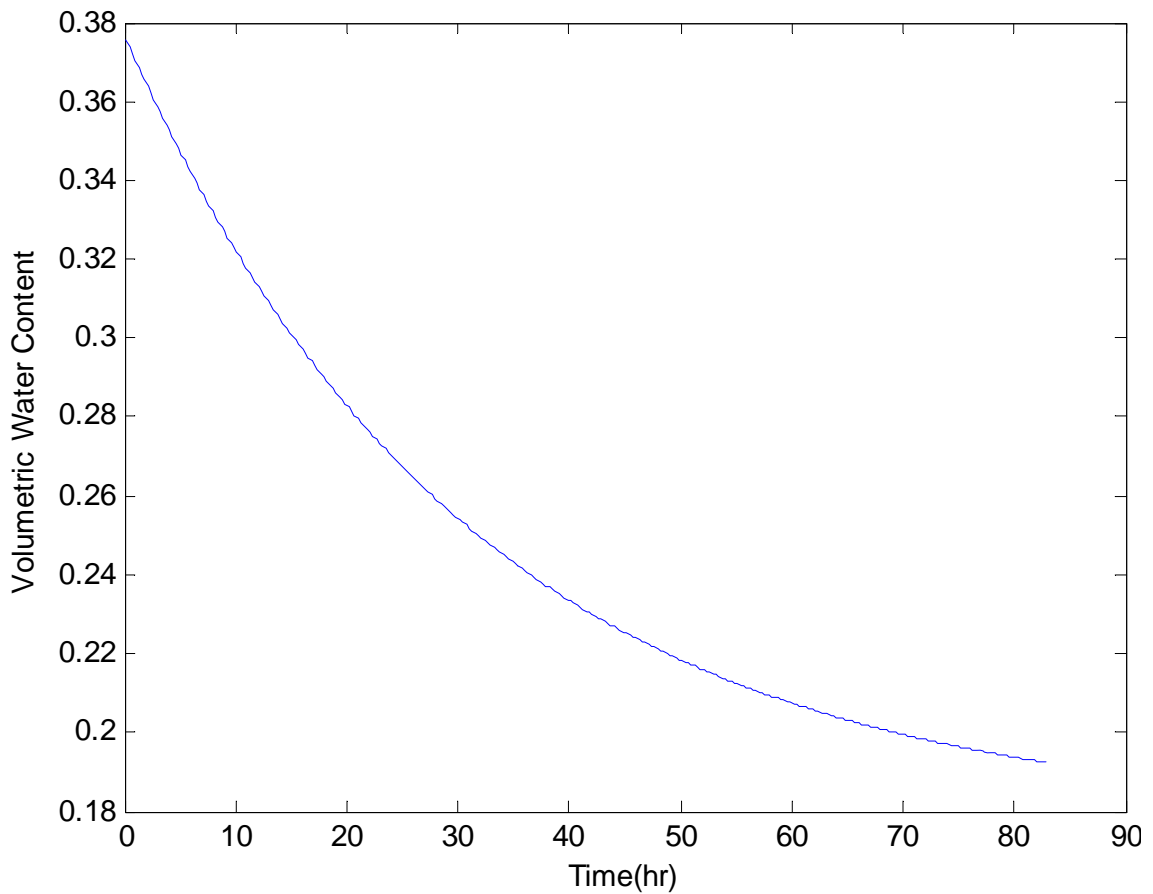the end of test, the volumetric water content is still around 20%.

Figure 15 Soil volumetric water content changes by time

From the evaporation rate vs. time and volumetric water content vs. time, the relationship between the evaporation rate and volumetric water content was calculated. Figure 16 Evaporation rate varies with the soil volumetric water contentshows how volumetric water content affects the evaporation rate during the test. The evaporation rate was high at the soil saturated condition, reaching 0.054g/s/m^2. After 84 hours it reduced to 0.005g/s/m^2. The curve fit is linear and approximated as $\dot{m} = 0.14\theta$ where θ is fractional moisture content and $\dot{m}$ soil evaporation rate in unit of g/s m^2.
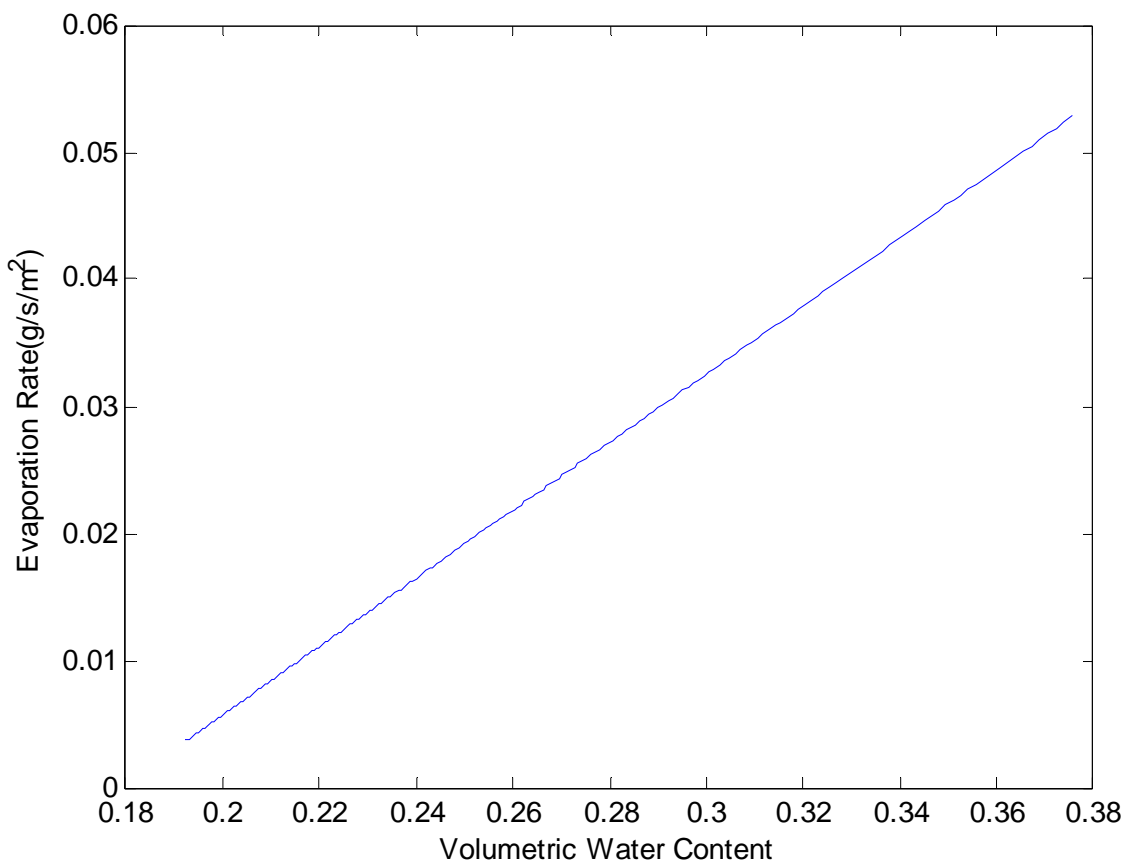

Figure 16 Evaporation rate varies with the soil volumetric water content

For soil layer heat conduction with no evaporation, the soil close to the surface should have a higher temperature than the soil beneath it. But if the soil surface has large moisture evaporation then Ts could be reduced by evaporative cooling. At this stage, from experiment the two functional dependencies needed for model testing were known,

$$K = 0.014 + 0.557\theta \tag{15}$$

$$\dot{m} = 0.14\,\theta \tag{16}$$

Using these equations, the model was tested to predict soil surface temperature T_S (θ) according to Equation 8 experimental histories of Ts, along with T_M and T_B, were recorded during dry out tests. These are shown in Figure 17 When the tray first entered the test wind tunnel, its temperature was uniform and approximately 19 °C; this was when the tray is still very moist, almost saturated. Within the first 4-5 hours, the soil temperature dropped at all three locations: top, middle, and bottom. This start-up phase, unavoidable as it was, affected the results for high-moisture readings. The temperature at the bottom dropped because of direct contact with the cold deck. The temperature at the surface dropped because it experienced large evaporative cooling, and then steadily increased throughout the 84-hour test period as the evaporative cooling diminished. The temperature at the center dropped as well, but not as much as would be expected since, once the transient effects were essentially complete, it should

have tracked approximately half way between the surface and the bottom. The recorded temperature at the middle appeared to be about 3-4 °C high throughout the duration of the test and has been adjusted in Figure 17 to demonstrate the probable curve. The reason for this discrepancy is unknown. Possible explanations include sensor misalignment (not actually located in the center), localized conduction through the wooden support structure holding the thermocouple in place, or a faulty thermocouple.
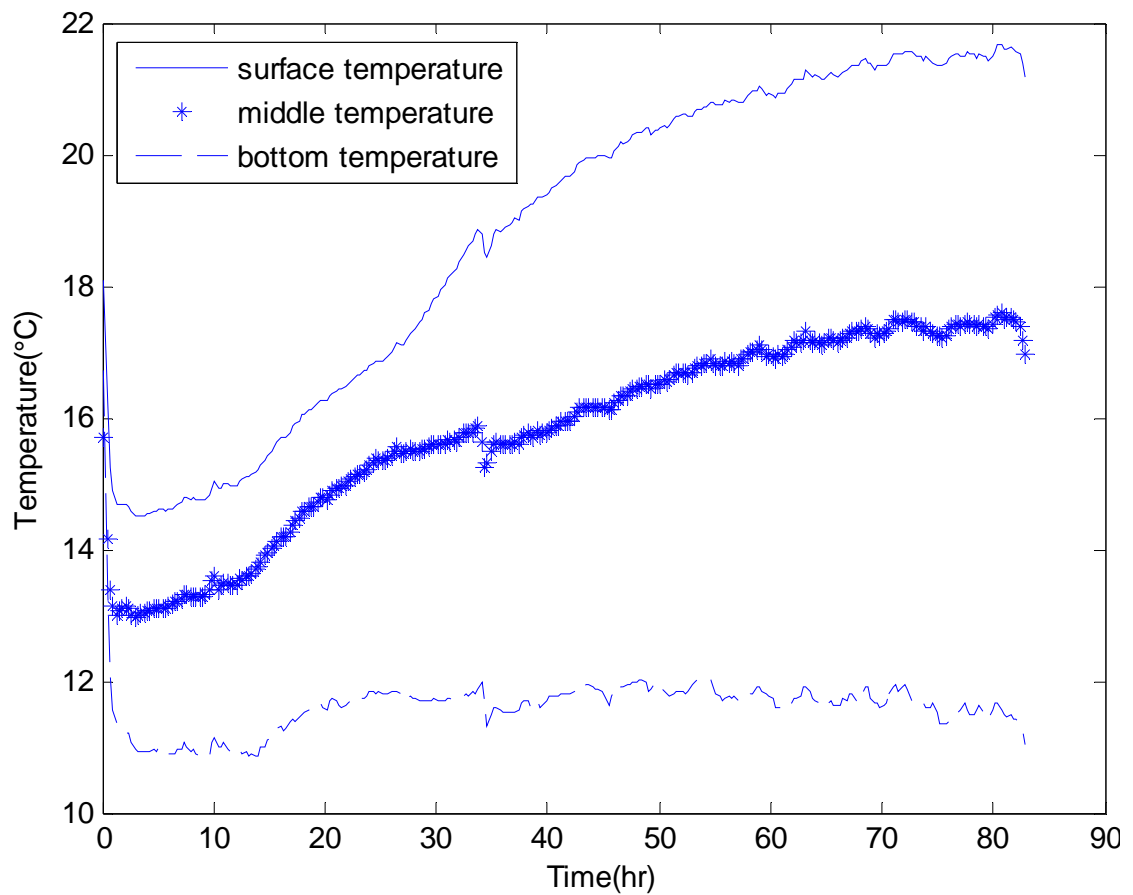

Figure 17 Three site soil temperature changes in dry out test

When the temperature change is converted from a time base to an average soil moisture base, as shown in Figure 18, the same trend is observed. The key point here is the dramatic change of surface temperature T_S with θ, changing almost 8°C for a moisture change from 035% to 20%.
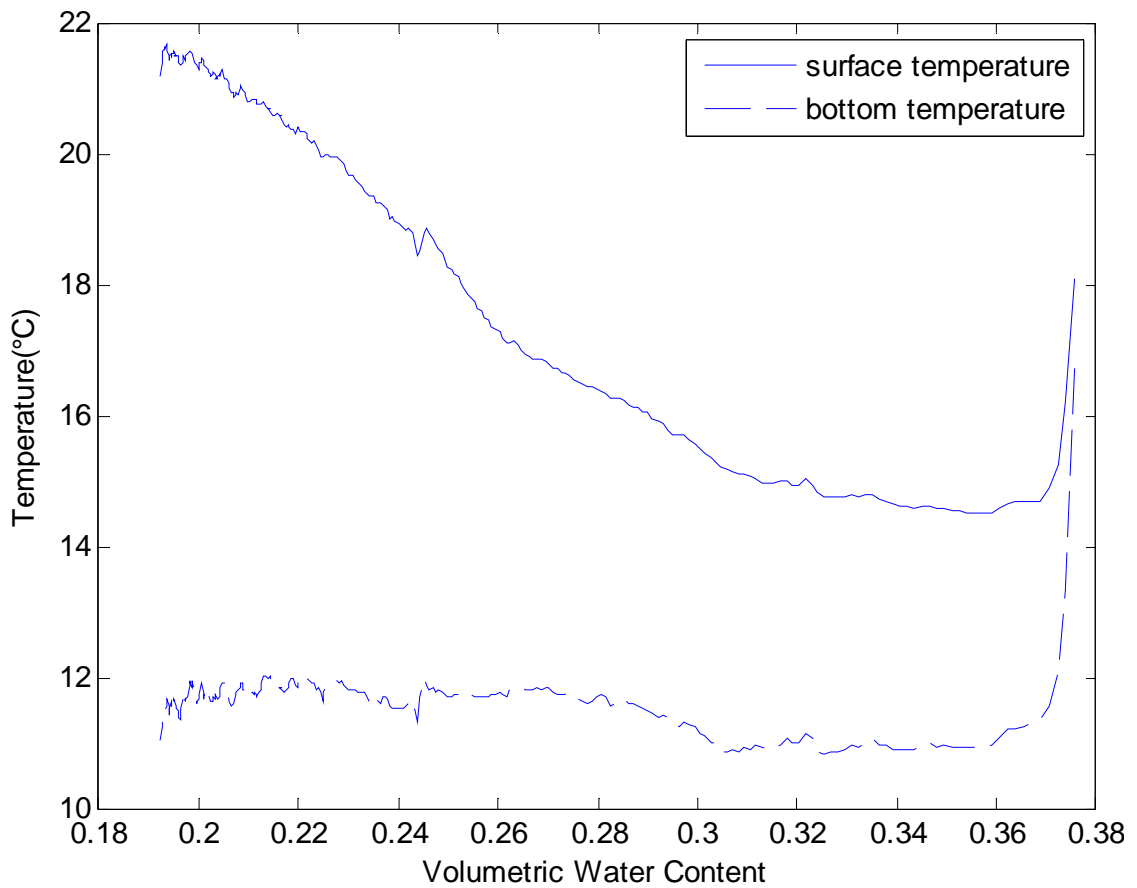

Figure 18 Soil surface and bottom temperature in different volumetric water content

Figure 19 shows the change of conductive heat flux at the bottom of the soil layer, as it changes with soil moisture. As the moisture content decreased, the heat flux went up. The heat flux range is from 78 to 112 W/m^2. The heat flux for θ>0.3, once again, was artificially high due to extreme temperature gradients at the tray bottom during start-up.

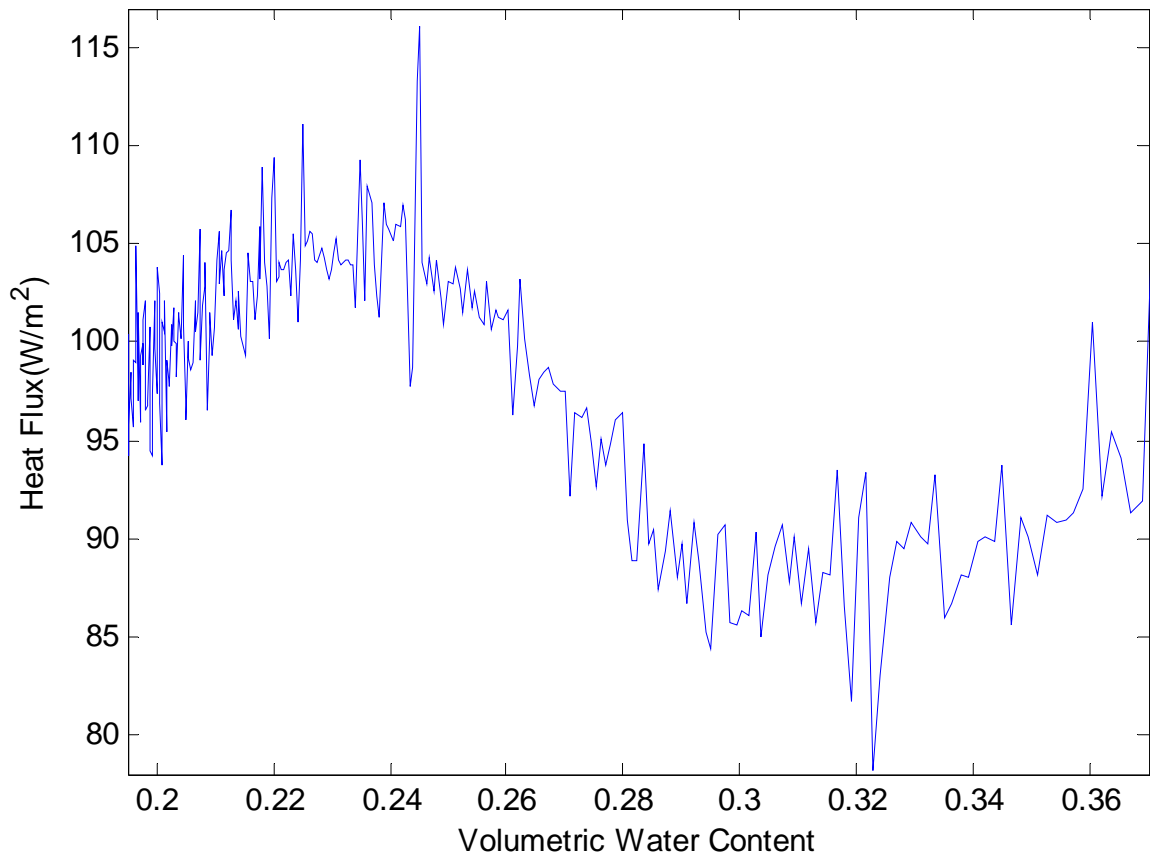Figure 19 Heal flux varied with volumetric water content in the test

During the test, a small amount of heat stored in the soil (as the soil lay is very thin). So the test is in a quasi-state condition. As a test of the validity of the quasi-static assumption, the following calculation was performed to make sure whether the model could ignore the heat storage term.

6.2 Theoretical analysis of soil layer thermal performance and its comparison with experimental results

From the test result, the soil water weight equation was

$$M = 38.33 + 9.33e^{-0.032t} \qquad (14)$$

The soil moisture time constant τ can be gotten from $M = Ce^{t/\tau}$. From the equation, τ is 31 hours.

For the time constant for heat storage is calculated by:

$$\tau_T = \frac{\rho L c_p}{h} \qquad (17)$$

Using ρ is 1220kg/m^3(Buccola and Spolek, 2010), L is 0.03m, $\overline{C}_p$ is 1070 J/kg K, and h is 4.22 W/m^2 K, τ_T is less than 3 hours, or about 1/10 that for moisture transfer.

From this calculation, the time constant of moisture transfer is one magnitude order of greater than that for heat transfer, meaning that the soil dries out much slower than heat transfer. The model assumption appears reasonable.

Using Equation 8 and the test data to calculate the convection coefficient h, the average h value is 4.22 W/m^{2}K

With the heat transfer coefficient of 4.22W/m^{2}K; soil depth was 0.03cm; thermal conductivity k value used Figure 12; bottom temperature T_B was the average actual data test during the experiment; a hot air temperature T_H set at 40 °C, and latent heat h_{fg} assume 2400 KJ/kg K. The model predicts the soil surface temperature. Figure 20 shows the model and experimental soil surface temperature as it changed with volumetric water content. The mathematical model predict T_S the surface temperature trend in reasonable agreement with the experiment. From the figure, the evaporative cooling clearly affects the soil surface temperature.
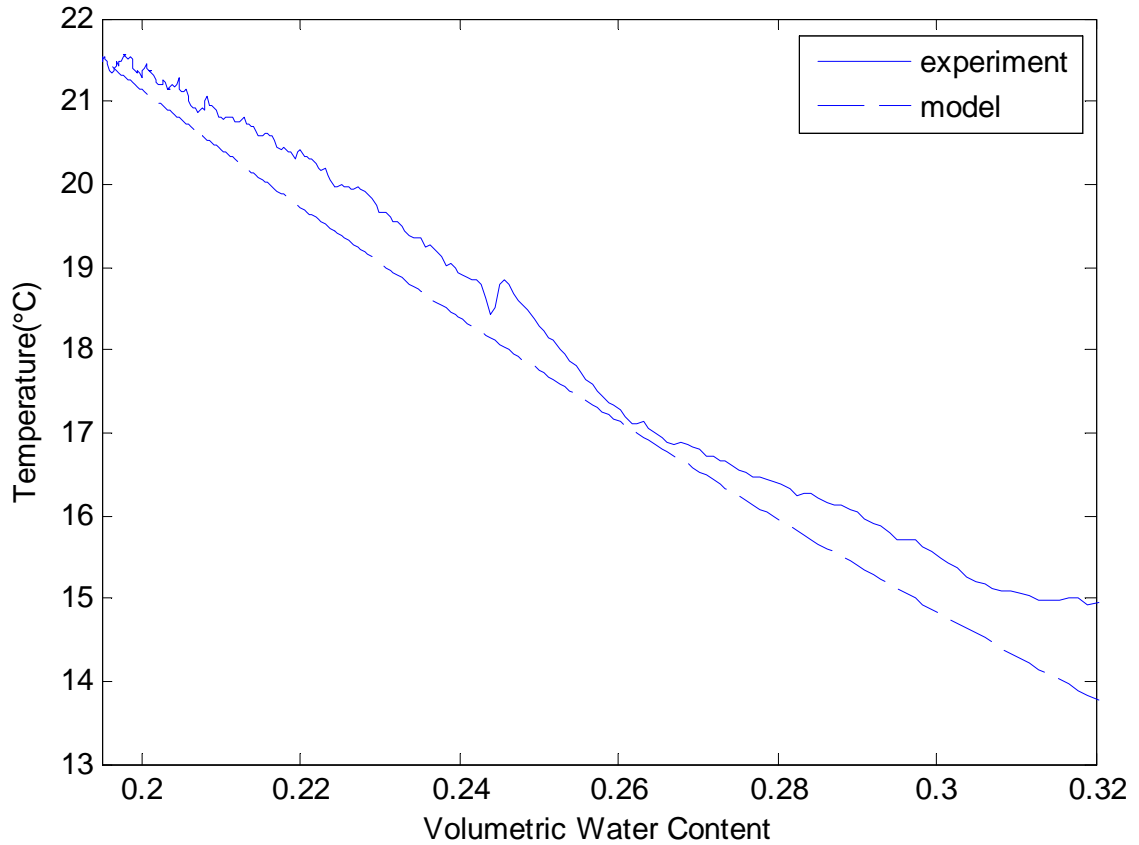
Figure 20 Comparison of the soil surface temperature in model value with experimental

one

Heat flux is calculated by $Q_{cond} = k \dfrac{T_S - T_B}{L}$, where Ts is model surface temperature, and

T$_B$ is average soil bottom temperature. Figure 21 shows the comparison of the heat flux

for model and experiment. The trend of both lines is similar, showing a decreased
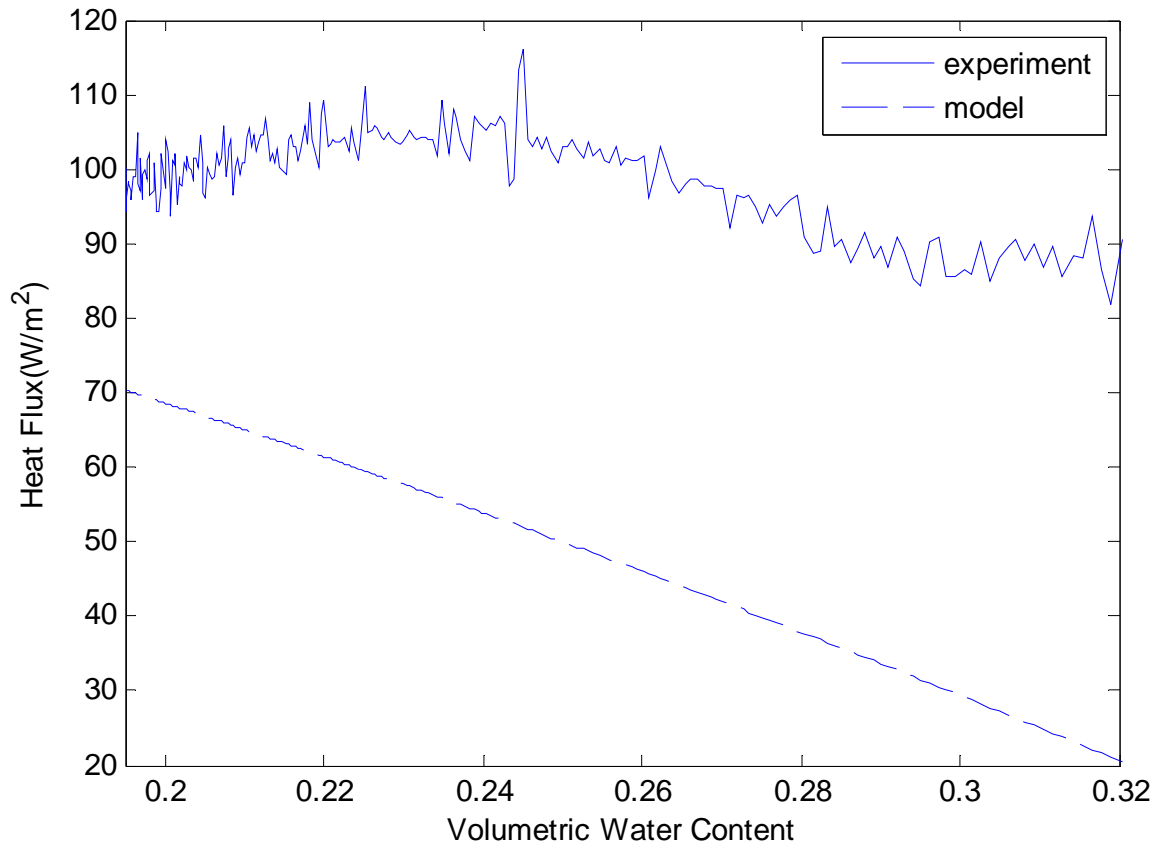
conductive heat flux with increased moisture.

Figure 21 Comparison of heat flux in experimental value with model value.

Conclusion

This study focus on how green roof thermal performance is affected by the soil moisture during summer conditions.

A predictive model was developed to include the major heat transfer processes including evaporative cooling. The soil substrate induces variation of thermal conductivity due to moisture content.

An experiment was designed and conducted to simulate a green roof soil layer, testing is thermal performance to validate the model. The experiment and the model show that the model predicts the model reasonably. Soil moisture is a very important factor in the green roof thermal performance, primarily due to the evaporative cooling effect that reduces the soil surface temperature in moist soil.

The basic research question, whether low conductivity for dry soil or high evaporation for moist soil has a greater impact on green roof performance, has been answered. Evaporation is more important. This result indicates that green roofs should be kept moist (irrigated) during hot weather to optimize building energy savings.

References

Alcazar ,S., Bass, B.(2005). Energy performance of green roofs in a-multi storey residential building in madrid. Greening Rooftops for Sustainable City Conference.

Becker, B. R., Misra, A., Fricke, B. A., (1992). Development of correlations for soil thermal conductivity. International Communications in Heat and Mass Transfer.19, 59-68

Bell, H., Spolek, G. (2009). Measured Energy Performance of Green Roofs. Paper presented at the Greening Rooftops for Sustainable Cities Conference.

Buccola, N., Spolek, G. (2010). A Pilot-Scale Evaluation of Green roof Runoff Retention, Detention, and Quality. Water, Air and Soil Pollution. 1-10

Curtis, O.F. (1936). Leaf temperatures and the cooling of leaves by radiation, Plant Physiology. 11 (2), 343 – 364.

Del Barrio, E. P. (1998). Analysis of the green roofs cooling potential in buildings. Energy

and Buildings 27(2). 179-193

Fang, C-F(2008). Evaluating the thermal reduction effect of plant layers on rooftops.

Energy and Building. 40, 1048-1052

Feng,C., Meng,Q. (2010). Theoretical and experimental analysis of the energy

balance of extensive green roofs.Energy and Buildings. 42 (6), 959–965.

KD2 Pro Specifications.(2006). Decagon Inc.

Kumar, R., Kaushik, R. C. (2005). Performance evaluation of green roof and shading for

thermal protection of building. Building and Environment. 40(11), 1505-1511

Lazzarin R. M., Castellotti F., & BusatoF. (2005). Experimental measurements and numerical modeling of a green roof. Energy and Buildings.37,1260-1267

Liu, K. (2003). Engineering performance of rooftop gardens through field evaluation NRCC-46294

Liu, K & B Baskaran, (2003), Thermal performance of green roofs through field evaluation, in Proceedings for the First North America Green Roof Infrastructure Conference: Greening Rooftops for Sustainable Communities, Chicago.

Medjelled A., Benchatti B., & Bouif A. (2008) Experimental model for the study of heat transfer in unsaturated soil: Case of underground thermal storage. International Journal of Heat and Technology.26, 97-104

Mellor, R.S., Salisbury, F.B., & Raschke, K. (1964). Leaf temperatures in controlled environment. Planta. 61(1), 56 – 72.

Ondimu, S N, Murase, H. (2007). Combining Galerkin methods and neural network analysis to inversely determine thermal conductivity of living green roof material. Biosystems Engineering. 96 (4), 541-550

Onmura, S. Matsumoto, M. Hokoi, S. (2001). Study on evaporative cooling effect of roof lawn gardens. Energy and Buildings. 33 (7), 653 – 666.

Perry, M.D. (2003). Green roofs offer environmentally friendly alternative. Plant Engineering. 57, 54

Philip,J.R.(1957). Evaporation, and moisture and heat fields in the soil. 14, 354-366

Sailor, D. (2008). A green roof model for building energy simulation programs. Energy and Buildings. 40, 1466-1478

Sailor, D., Hutchinson, D., Bokovoy, L. (2008). Thermal property measurements for ecoroof soils common in the western U.S.. Energy and Buildings. 40(7), 1246-1251

Spolek, G. (2008). Performance monitoring of three ecoroofs in Portland, Oregon. Urban Ecosystems, 11(4), 349-359.

Suleiman, A. A., Ritchie, J. T. (2003). Modeling soil water redistribution during second-stage evaporation. Soil Science Society of America Journal, 67(2), 377-386

Tabares-velasco. (2009). Heat fluxes and water management of a green and brown roof: laboratory experiments, in: Greening Rooftops for Sustainable Communities

Takakura, T. ,Kitade, S., & Goto, E.(2000). Cooling effect of greenery cover over a building, Energy and Buildings. 31, 1-6

Theodosiou, T. G. (2003). Summer period analysis of the performance of a planted roof as a passive cooling technique, Energy and Buildings. 35 (9), 909–917.

Theodore, O. (1999). Roof Gardens: History, Design and Construction. New York: W.W. Norton & Company Inc.

Green Roof Industry Survey Results in 2008,

http://www.greenroofs.org/index.php/mediaresource/industry-survey-2008

Wong, N.H., Chen, Y., Ong, C.L., Sia, A. (2003).Investigation of thermal benefits of

rooftop garden in the tropical environment. Building and Environment. 38 (4), 261 – 270.

Wong, N. H., Cheong, D. K. W., Yan, H., Soh, J., Ong, C. L, Sia, A. (2002). The effects of

rooftop garden on energy consumption of a commercial building in Singapore. Energy

and Buildings. 35, 353-364